Table S1. Electronic (***g*** Tensor) Parameters for Ni(I) and Ni(III) Complexes Relevant to MCR.

Complex[a]	$g = [g_1, g_2, g_3]$[b]	References and Notes
MCRred1	2.2485(5), 2.070(1), 2.060(1) 2.260, 2.088, 2.088	This work, 35 GHz Ref. 43
MCRox1	2.229(2), 2.166(2), 2.148(2) 2.227, 2.159, 2.159	This work, 35 GHz Ref. 43
MCRox2	2.227(2), 2.140(5), 2.125(5)	This work, 35 GHz
$Ni^{I}F_{430}$	2.244, 2.063, 2.063 2.224, 2.061, 2.061	Ref. 13, 35 GHz Ref. 26
$Ni^{I}F_{430}Me_5$	2.250, 2.074, 2.065	Ref. 44 [c]
Ni^{I}OEiBC	2.204, 2.080, 2.063 2.2025, 2.083, 2.061	Ref. 13, 35 GHz[d] Ref. 45 [d]
$Ni^{I}Me_6$[14]1,4,8,11-tetraeneN_4	2.195, 2.053, 2.053	Ref. 9 [e]
$Ni^{I}Me_6$[14]4,11-dieneN_4	2.226, 2.055, 2.055	Ref. 9 [e]
$Ni^{I}Me_6$[14]aneN_4	2.261, 2.060, 2.060	Ref. 9 [e]
$Ni^{III}F_{430}$	2.020, 2.211, 2.211	Ref. 8 [e]
$Ni^{III}Me_6$[14]1,4,8,11-tetraeneN_4	2.018, 2.186, 2.186	Ref. 9 [e]
$Ni^{III}Me_6$[14]4,11-dieneN_4	2.024, 2.199, 2.199 2.021, 2.232, 2.232	Ref. 9 [e] Ref. 46
$Ni^{III}Me_6$[14]aneN_4	2.029, 2.215, 2.215 2.028, 2.238, 2.238	Ref. 9 [e] Ref. 46
$Ni^{III}(Me_2$[14]ane$N_4)(NCO)_2$	2.055, 2.169, 2.169	Ref. 24 [f]
Ni^{III}[14]aneN_4	2.0332, 2.2193, 2.2193	Ref. 23

Ni^{III}[14]ane$N_4(NCS)_2$	2.02(1), 2.14(1), 2.14(1)	Ref. 23 [g]
$Ni^{III}TPP(thf)_2$	2.093, 2.328, 2.305	Ref. 34 [h]
$Ni^{III}TPP(CN)_2$	2.178, 2.065, 2.045	Ref. 34 [h]
$Ni^{III}DAPA(SPh)_2$	2.03, 2.21, 2.21	Ref. 32 [i]
$Ni^{I}DAPA(SPh)_2$	2.26, 2.14, 2.09	Ref. 32 [i]

[a]Abbreviations used: DAPA, 2,6-bis[(1-phenylimino)ethyl]pyridine; F_{430}, nickel tetrapyrrole pentacarboxylic acid cofactor; $F_{430}Me_5$, nickel tetrapyrrole pentamethyl ester cofactor; MCR, methyl-coenzyme M reductase; [14]aneN_4, 1,4,8,11-tetraazacyclotetradecane (commonly known as cyclam); Me_2[14]aneN_4, 2,3-dimethyl-1,4,8,11-tetraazacyclotetradecane; Me_6[14]1,4,8,11-tetraeneN_4, 5,7,7,12,14,14-hexamethyl-1,4,8,11-tetraazacyclotetradeca-1,4,8,11-tetraene; Me_6[14]4,11-dieneN4, 5,7,7,12,14,14-hexamethyl-1,4,8,11-tetraazacyclotetradeca-4,11-diene; OEiBC, octaethylisobacteriochlorin (*tct*-2,3,7,8-tetrahydro-2,3,7,8,12,13,17,18-octaethylporphyrin dianion); thf, tetrahydrofuran; TPP, 5,10,15,20-tetraphenylporphyrin dianion.

[b]All g values were determined at X-band (~9 GHz), except as otherwise noted. The X-band studies reported axial EPR spectra in all cases. For comparison with the rhombic spectra resolved at Q-band (35 GHz), the g values are given in the order $[g_z, g_y, g_x]$, where $g_z \equiv g_\perp$ and $g_x = g_y \equiv g_\parallel$ for axial systems; and $g_y \equiv g_{mid}$, $g_x \equiv g_{min}$ for rhombic systems. All samples were in frozen aqueous solution, except as otherwise noted. X-band spectra were recorded at 60 - 100 K; 35 GHz spectra at 2 K.

[c]In tetrahydrofuran frozen solution.

[d]In 2-methyltetrahydrofuran frozen solution.

[e]In acetonitrile frozen solution.

[f]Powder sample; similar *g* values obtain with other bisaxial ligands (Br^-, Cl^-, NO_3^-).

[g]*g* values estimated here from Figure 5 in Ref. 23, which did not report the *g* values. Hyperfine coupling to two equivalent nitrogen ligands is resolved.

Table S2. Hyperfine and Quadrupole Couplings for Equatorial Nitrogen Ligands in $d^{9,7}$ Macrocyclic Complexes Relevant to F_{430}.

Complex[a]	$A(^{14}N) = [A_1, A_2, A_3]$ (MHz)[b]	$P(^{14}N) = [P_1, P_2, P_3]$ (MHz)[b]
MCRred1, $N_{1,3}$ [c]	36(1), 27(1), 30.6(4)	-1.2(2), 0.8(2), 0.4(2)
MCRred1, $N_{2,4}$ [c]	31.5(5), 22.5(5), 25.0(5)	-1.8(2), 1.5(2), 0.3(2)
MCRox1, N_1 [c]	31(1), 22(1), 24(1)	-1.6(2), 1.0(2), 0.6(2)
MCRox1, N_2 [c]	31.5(1.0), 24.5(1.0), 21(1)	-1.3(2), 0.7(2), 0.6(2)
MCRox1, N_3 [c]	33(1), 24(1), 24.5(1.0)	-1.6(2), 1.0(2), 0.6(2)
MCRox1, N_4 [c]	33.5(1.0), 26.5(1.0), 26.3(5)	-1.3(2), 0.7(2), 0.6(2)
MCRox2, $N_{1,3}$ [c]	31.5(1.0), 25.0(1.0), 24.0(1.0)	-1.3(2), 1.0(2), 0.3(2)
MCRox2, $N_{2,4}$ [c]	34.7(5), 27.7(5), 27.5(1.0)	-1.4(2), 1.0(2), 0.4(2)
Ni^{I}OEiBC $N_{1,3}$ [d]	33.0(5), 29.0(5), 25.0(0.2)	-1.50(10), 0.90(10), 0.60(5)
Ni^{I}OEiBC $N_{2,4}$ [d]	35.0(5), 27.0(5), 25.0(0.2)	-1.00(10), 0.40(10), 0.60(5)
$Ni^{I}F_{430}$ $N_{1,3}$ [e]	31(1), 22(1), 26.5(0.5)	-1.85(20), 1.10(20), 0.75(5)
$Ni^{I}F_{430}$ $N_{2,4}$ [e]	34(1), 27(1), 26.5(0.5)	-1.35(20), 0.60(20), 0.75(5)
Cu^{II}TPP [f]	54.213, 42.778, 44.065	-0.619, 0.926, -0.307
Ni^{III}TPP$(thf)_2$ [g]	0.0	not reported
Ni^{III}TPP$(CN)_2$ [g]	38, 41, 41	not reported
Co^{II}TPP(py) [g]	4.07, 2.85, 2.43	-0.90, 0.70, 0.20
$Co^{II}(dmg)_2(py)$ [h]	2.61, 1.86, 1.84	-1.70, 1.45, 0.25
Ni^{III}14aneN_4 [i]	≤ 6	not resolved

[a]Abbreviations used: dmg, dimethylglyoxime anion; F_{430}, nickel tetrapyrrole pentacarboxylic acid cofactor; MCR, methyl-coenzyme M reductase; OEiBC, octaethylisobacteriochlorin (*tct*-2,3,7,8-tetrahydro-2,3,7,8,12,13,17,18-octaethylporphyrin dianion); py, pyridine; thf, tetrahydrofuran; TPP, 5,10,15,20-tetraphenylporphyrin dianion.

[b]The coordinate system is such that $\boldsymbol{A}(^{14}N)$ and $\boldsymbol{P}(^{14}N)$ are collinear and related to $\boldsymbol{g}$ by Euler angles $\alpha = 0$, $\beta = 90$, $\gamma = 45°$, so that $(A, P)_1$ is along the metal-nitrogen bond, $(A, P)_2$ is in-plane, normal to the metal-nitrogen bond (so that $(A, P)_{1,2}$ lie exactly between g_2 and g_3), and $(A, P)_3$ is normal to the macrocycle plane (along g_1).

[c]This work; in aqueous ethylene glycol (~30% v/v) frozen solution.

[d]In 2-methyltetrahydrofuran frozen solution.[13] The values reported here differ slightly from those originally reported due to more extensive examination of multiple data sets for Ni(I)OEiBC.

[e]In aqueous ethylene glycol (~55% v/v) frozen solution.[13]

[f]Doped into Zn(II)TPP single-crystal; values determined by ENDOR.[18]

[g]In dichloromethane frozen solution; values determined by EPR.[34]

[g]In toluene frozen solution; values determined by ESEEM and ENDOR.[20]

[h]In methanol/toluene frozen solution; values determined by ESEEM.[19]

[i]Generated by addition of $(NH_4)_2S_2O_8$ to aqueous Ni(II)[14]aneN_4Cl_2 (following Ref. 24). 35 GHz ENDOR showed only a roughly isotropic signal at 3 - 5 MHz, which would give a maximum coupling of $A(^{14}N) = 6$ MHz, based on an assignment to the ν_+ partner of a pattern centered at $A(^{14}N)/2$.

A Ni(II)F_{430}, $S_1 = 1$, spin-coupled to a (thiyl) radical, $S_2 = 1/2$, to give a total spin, $S_t = 1/2$, has $\boldsymbol{g}' = (4/3)\boldsymbol{g}_1 - (1/3)\boldsymbol{g}_2$, where $\boldsymbol{g}'$ is the observed $\boldsymbol{g}$ matrix for the coupled system and $\boldsymbol{g}_1$ and $\boldsymbol{g}_2$ are those for the uncoupled species. For a nucleus with an intrinsic hfc given by $\boldsymbol{a}_1$ (~30 MHz for ^{14}N in an authentic $d_{x^2-y^2}{}^1$ species, such as Ni(I)OEiBC and Ni(I)F_{430}), the observed hfc in the coupled system is $\boldsymbol{A}_1' = (4/3)\boldsymbol{A}_1 = (4/3)(\boldsymbol{a}_1/2S_1) = (4/3)(30/2) = 20$ MHz, where $\boldsymbol{A}_1$ is the hfc in the $S_1 = 1$ uncoupled system.

Yet another suggestion, that the "ox" states are EPR-visible Ni(II), S = 1, is not credible: the EPR signals are not characteristic of $S = 1$ and the ligand field in F_{430} would in any case cause axial zero field splittings that are too large to allow observation of X-band EPR spectra.[35]

Rospert, S.; Voges, M.; Berkessel, A.; Albracht, S. P. J.; Thauer, R. K. *Eur. J. Biochem.* **1992**, *210*, 101-107.

Jaun, B.; Pfaltz, A. *J. Chem. Soc., Chem. Commun.* **1986**, 1327-1329.

Renner, M. W.; Furenlid, L. R.; Stolzenberg, A. M. *J. Am. Chem. Soc.* **1995**, *117*, 293-300.

Zeigerson, E.; Ginzburg, G. *J. Chem. Soc., Chem. Commun.* **1979**, 241-243.

Figure Captions.

S1. Experimental (upper trace of pair) and simulated (lower trace of pair) 35 GHz EPR spectra of **A**) Ni(I)OEiBC; **B**) isolated Ni(I)F_{430}; **C**) MCRox2; **D**) MCRox1. The spectra were recorded using the dispersion mode under passage conditions; a digital first derivative is shown. The abscissa is in *g* value to facilitate comparison among spectra. The EPR spectrum of MCRred1 is not shown here, but is shown in Figure 2 and is almost identical to that of Ni(I)F_{430}. Experimental conditions: **A**) upper trace: *tct*-Ni(I)OEiBC, generated by reduction of Ni(II)OEiBC using Na(Hg) amalgam, 0.5 mM in 2-Me-THF; temperature, 2 K; microwave frequency, 35.422 GHz; microwave power, 2 mW; 100 kHz field modulation amplitude, 0.03 mT; time constant, 32 ms; lower trace: simulation using: $g_z = 2.204$, $g_y = 2.080$, $g_x = 2.063$; Gaussian linewidths (hwhm): W_z = 155 MHz, $W_{x,y}$ = 100 MHz. **B**) upper trace: Ni(I)F_{430}, generated by reduction of F_{430} using Ti(III)citrate, 0.25 mM in 0.1 *M*, pH= 10.4 CAPS buffer with 55% (v/v) ethylene glycol; instrument parameters as in (A) except: microwave frequency, 35.035 GHz; microwave power, 2 μW; modulation amplitude, 0.1 mT; lower trace: simulation using $g_{\|} = 2.244$, $g_{\perp} = 2.063$; $W_{\|}$ = 140 MHz, $W_{\perp}$ = 90 MHz. For comparison, simulation of MCRred1 used: $g_z = 2.2485$, g_y = 2.070, $g_x = 2.060$; W_{iso} = 80 MHz. **C**) upper trace: MCRox2; 0.71 mM; 50 mM Tris-HCl, pH 7.6; instrument parameters as in (B) except: microwave frequency, 34.931 GHz; microwave power, 20 μW; lower trace: simulation using: $g_x = 2.125$, $g_y = 2.140$, $g_z = 2.227$; W_{iso} = 90 MHz. **D**) upper trace: MCRox1; 0.60 mM; 50 mM, pH 7.6 buffer; instrument parameters as in (C) except: microwave frequency, 34.968 GHz; lower trace: simulation using: $g_x = 2.148$, $g_y = 2.166$, $g_z = 2.229$; W_{iso} = 75 MHz.

S2. Qualitative d orbital scheme for d^7 (low-spin) and d^9 complexes. Electron occupancies common to both d^7 and d^9 are unmarked, while those exclusive to d^7 are circled and those exclusive to d^9 are boxed.

S3. Experimental (upper trace of pair) and simulated (lower trace of pair) field dependent 35 GHz CW ^{14}N ENDOR spectra for MCRox1. Experimental conditions: protein concentration, 0.60 mM; 50 mM Tris-HCl, pH 7.6; **A**) temperature, 2 K; microwave frequency, 34.970 GHz; microwave power, 13 μW (42 dBm); magnetic field, 1.1250 T (g = 2.221); 100 kHz field modulation amplitude, 0.3 mT; time constant, 64 ms; rf scan rate, -0.5MHz/s; average rf power, 5 W; 20 scans. **B**) same as (**A**) except: magnetic field, 1.1360 T (g = 2.199); **C**) same as (**A**) except: magnetic field, 1.1460 T (g = 2.180); **D**) same as (**A**) except: magnetic field, 1.1590 T (g = 2.156; corresponding to $g = [(g_2^2 + g_3^2)/2]^{1/2}$); **E**) same as (**A**) except: magnetic field, 1.1620 T (g = 2.150); **F**) same as (**A**) except: magnetic field, 1.1650 T (g = 2.145); Simulation parameters: $\boldsymbol{g}$ = [2.229, 2.166, 2.148]; sum of equal weights of the following four types of nitrogen ligand, N_n, n = 1, 4: $\boldsymbol{A}(^{14}N_1)$ = [33.5, 26.5, 26.3] MHz, $\boldsymbol{P}(^{14}N_1)$ = [-1.3, 0.7, 0.6] MHz; $\boldsymbol{A}(^{14}N_2)$ = [33.0, 24.0, 24.4] MHz, $\boldsymbol{P}(^{14}N_2)$ = [-1.6, 1.0, 0.6] MHz; $\boldsymbol{A}(^{14}N_3)$ = [31.5, 24.5, 21.0] MHz, $\boldsymbol{P}(^{14}N_1)$ = [-1.3, 0.7, 0.6] MHz; $\boldsymbol{A}(^{14}N_4)$ = [31.0, 22.0, 24.0] MHz, $\boldsymbol{P}(^{14}N_4)$ = [-1.6, 1.0, 0.6] MHz. The $\boldsymbol{A}(^{14}N_1)$ and $\boldsymbol{P}(^{14}N_1)$ tensors are related to the $\boldsymbol{g}$ tensor by the following Euler angle rotations: $\alpha = 0^\circ$, $\beta = 90^\circ$, $\gamma = (45 + 90(n - 1))^\circ$, where n = 1, 4 (nitrogen ligand identifier). In all cases the following Gaussian linewidths (hwhh) are used: EPR, 75 MHz; ENDOR, 0.35 MHz.

S4. Experimental (upper trace of pair) and simulated (lower trace of pair) field dependent 35 GHz CW ^{14}N ENDOR spectra for MCRox2. Experimental conditions: protein concentration, 0.71 mM; 50 mM Tris-HCl, pH 7.6; **A**) temperature, 2 K; microwave frequency, 34.958 GHz; microwave power, 20 μW (40 dBm); magnetic field, 1.1250 T (g = 2.220); 100 kHz field modulation amplitude, 0.3 mT; time constant, 64 ms; rf scan rate, -1MHz/s; average rf power, 5 W; 30 scans. **B**) same as (**A**) except: magnetic field, 1.1350 T (g = 2.200); **C**) same as (**A**) except: magnetic field, 1.1460 T (g = 2.179); **D**) same as (**A**) except: magnetic field, 1.1560 T (g = 2.161); **E**) same as (**A**) except: magnetic field, 1.1700 T (g = 2.135; corresponding to $g = [(g_2^2 + g_3^2)/2]^{1/2}$); **F**) same as (**A**) except: magnetic field, 1.1780 T (g = 2.120); Simulation parameters: $\boldsymbol{g}$ = [2.227, 2.140, 2.125]; sum of equal weights of the following four nitrogen ligands in two distinct types, N_n, n = 1, 4: $\boldsymbol{A}(^{14}N_{1,3})$ = [34.7, 27.7, 28.5] MHz, $\boldsymbol{P}(^{14}N_{1,3})$ = [-1.3, 1.0, 0.3] MHz; $\boldsymbol{A}(^{14}N_{2,4})$ = [31.5, 25.0, 25.5] MHz, $\boldsymbol{P}(^{14}N_{2,4})$ = [-1.4, 1.0, 0.4] MHz. The $\boldsymbol{A}(^{14}N_1)$ and $\boldsymbol{P}(^{14}N_1)$ tensors are related to the $\boldsymbol{g}$ tensor by the following Euler angle rotations: $\alpha = 0°$, $\beta = 90°$, $\gamma = (45 + 90(n - 1))°$, where n = 1, 4 (nitrogen ligand identifier). In all cases the following Gaussian linewidths (hwhh) are used: EPR, 75 MHz; ENDOR, 0.35 MHz.

S5. Experimental (upper trace of pair) and simulated (lower trace of pair) field dependent 35 GHz CW ^{14}N ENDOR spectra for MCRred1. Experimental conditions: protein concentration, 0.48 mM; Ti(III)citrate, 40 mM; 0.5 M TAPS buffer, pH 10.0; **A**) temperature, 2 K; microwave frequency, 34.919 GHz; microwave power, 20 μW (40 dBm); magnetic field, 1.1140 T (g =

2.240); 100 kHz field modulation amplitude, 0.3 mT; time constant, 32 ms; rf scan rate, -0.5 MHz/s; average rf power, 5 W; 40 scans. **B**) same as (**A**) except: magnetic field, 1.1660 T (g = 2.140); **C**) same as (**A**) except: magnetic field, 1.1770 T (g = 2.120); **D**) same as (**A**) except: magnetic field, 1.1880 T (g = 2.100); **E**) same as (**A**) except: magnetic field, 1.1990 T (g = 2.081; **F**) same as (**A**) except: magnetic field, 1.2050 T (g = 2.070); Simulation parameters: $\boldsymbol{g}$ = [2.2485, 2.070, 2.060]; sum of equal weights of the following four nitrogen ligands in two distinct types, N_n, n = 1, 4: $\boldsymbol{A}(^{14}N_{1,3})$ = [36.0, 27.0, 30.6] MHz, $\boldsymbol{P}(^{14}N_{1,3})$ = [-1.2, 0.8, 0.4] MHz; $\boldsymbol{A}(^{14}N_{2,4})$ = [31.5, 22.5, 25.0] MHz, $\boldsymbol{P}(^{14}N_{2,4})$ = [-1.8, 1.5, 0.3] MHz. The $\boldsymbol{A}(^{14}N_1)$ and $\boldsymbol{P}(^{14}N_1)$ tensors are related to the $\boldsymbol{g}$ tensor by the following Euler angle rotations: $\alpha = 0°$, $\beta = 90°$, $\gamma = (45 + 90(n - 1))°$, where n = 1, 4 (nitrogen ligand identifier). In all cases the following Gaussian linewidths (hwhh) are used: EPR, 75 MHz; ENDOR, 0.35 MHz.

S6. Experimental (top trace) and simulated (middle and bottom traces) 35 GHz EPR spectrum of MCR treated with excess Ti(III)citrate showing the simultaneous presence of MCRox1 and MCRred1. Experimental conditions are given in Figure 1 for MCRred1. EPR simulation parameters are given in Table 1. The EPR spectrum exhibits ox1 and red1 with comparable signal intensities; not shown is the vastly greater (~100x) signal at higher field due to unreacted Ti(III)citrate.

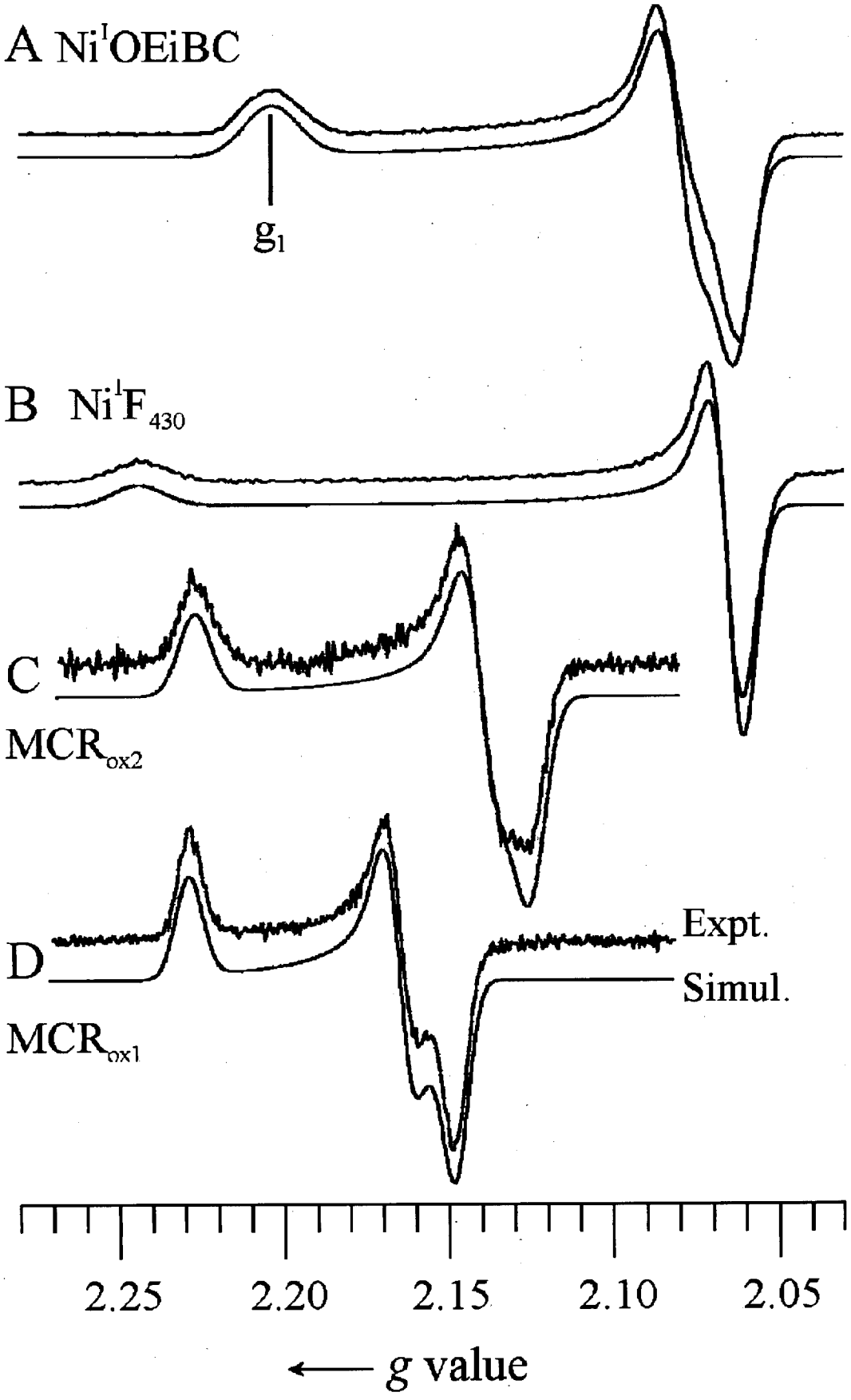

Fig. S1, Telser et al.

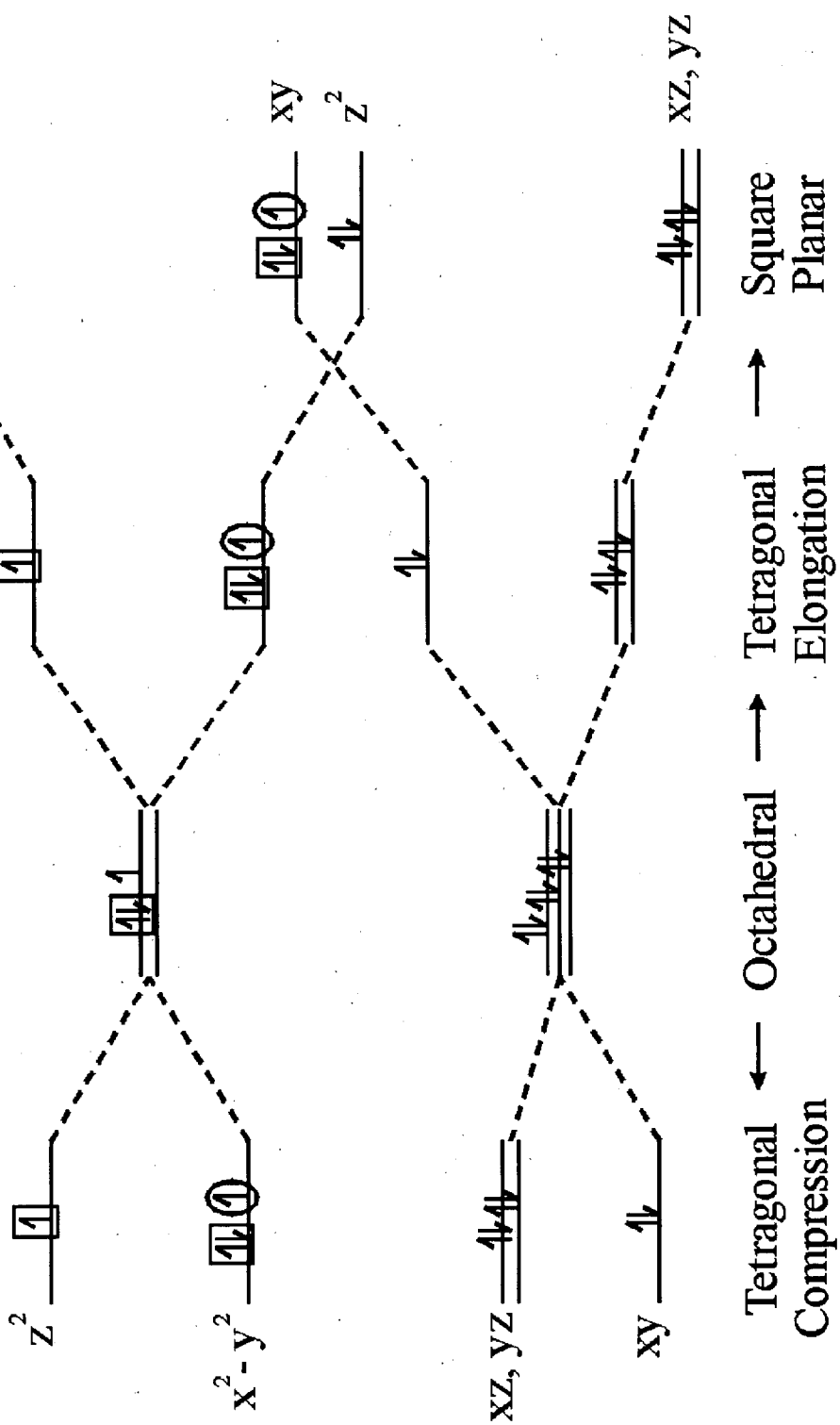

Fig. S2, Telser et al.

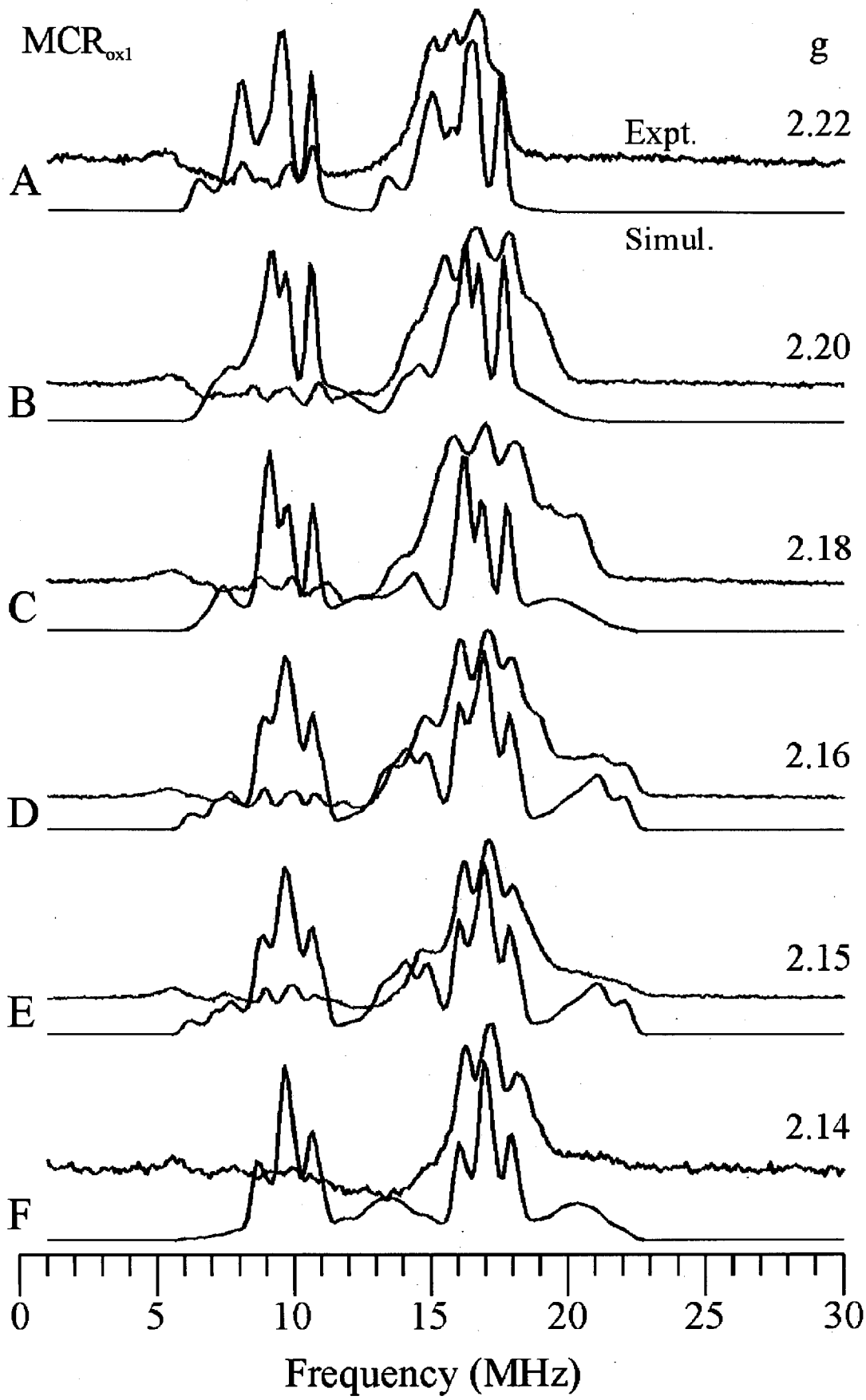

Fig. S3, Telser et al.

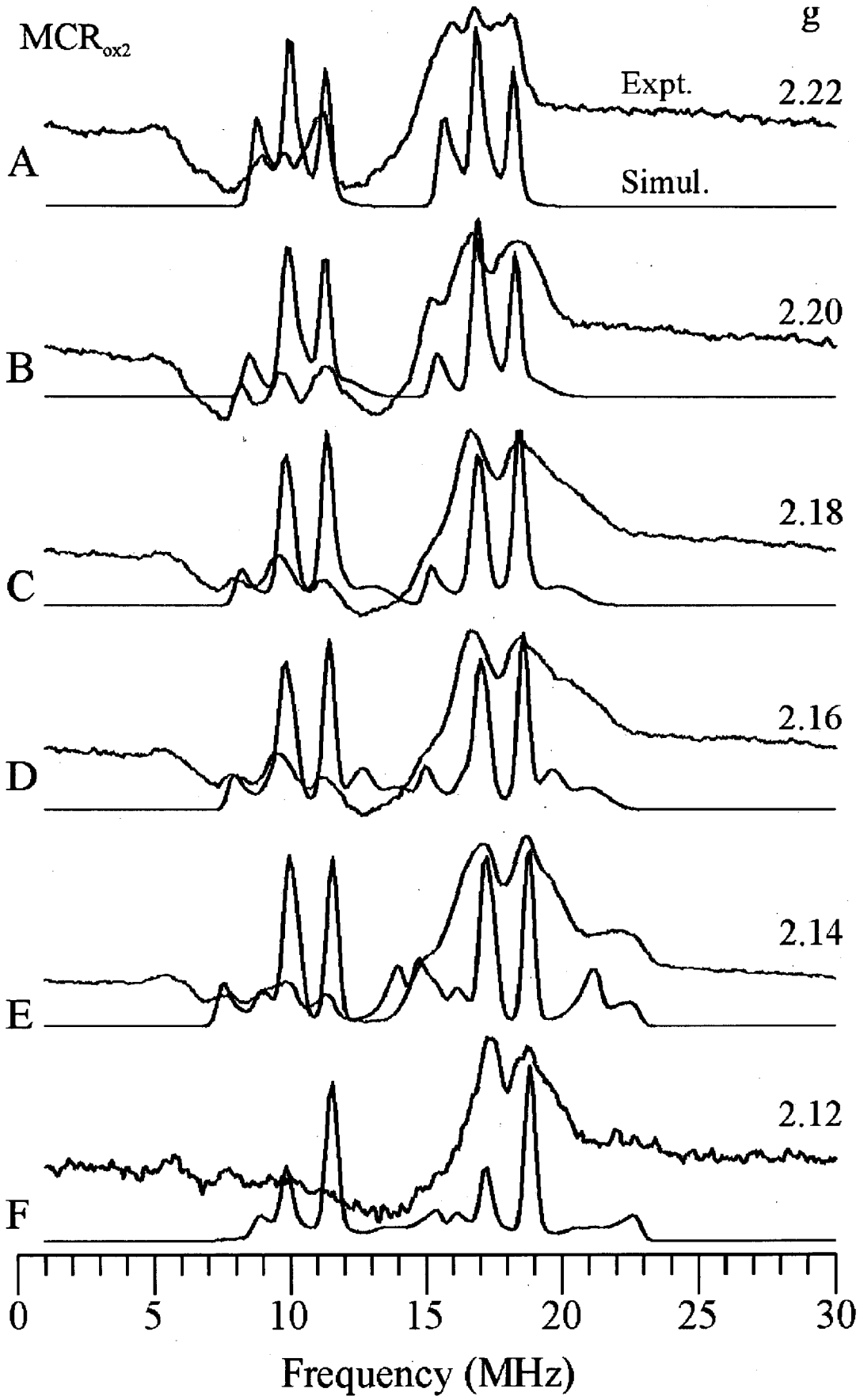

Fig. S4, Telser et al.

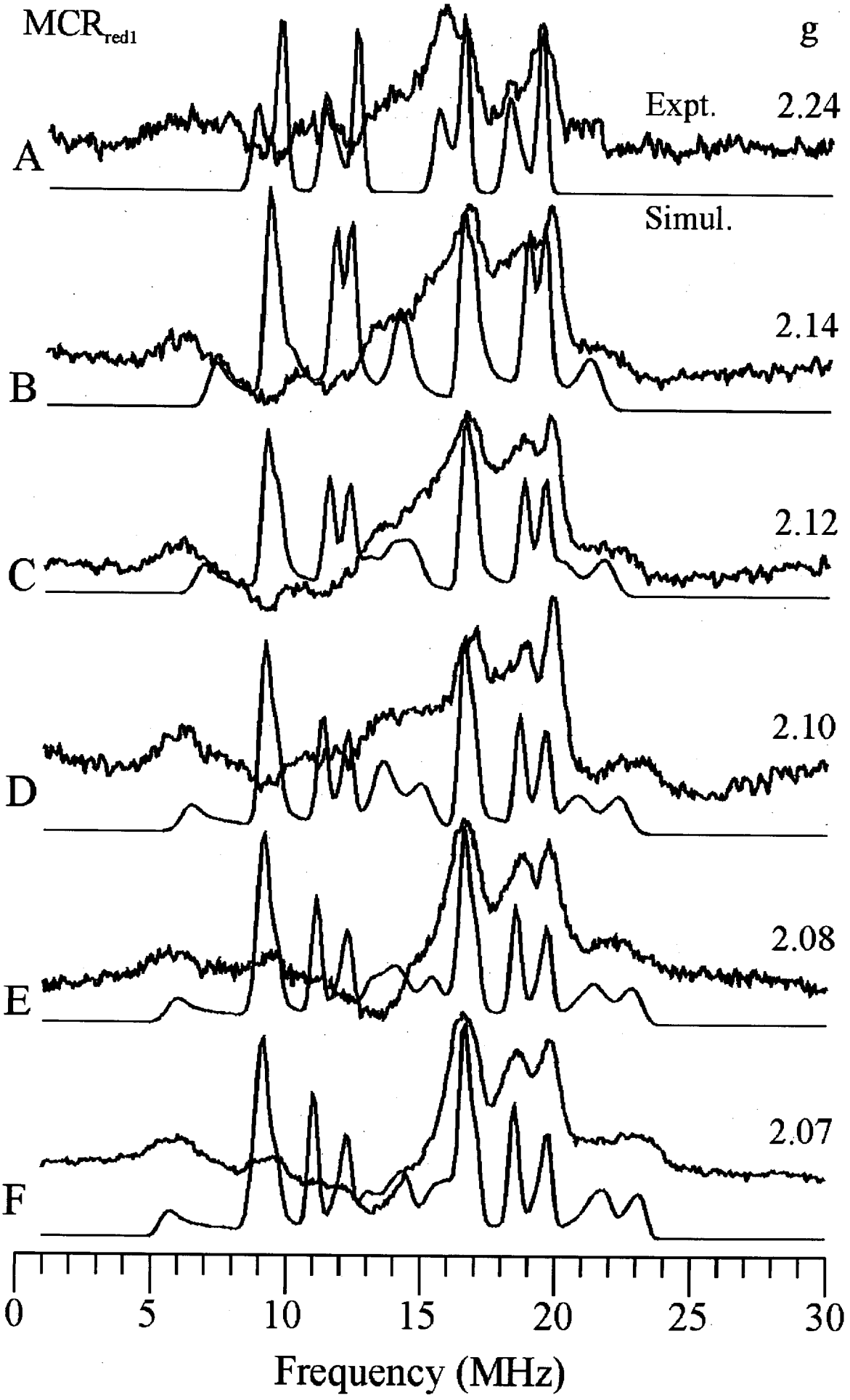

fig S5 Telser et al.

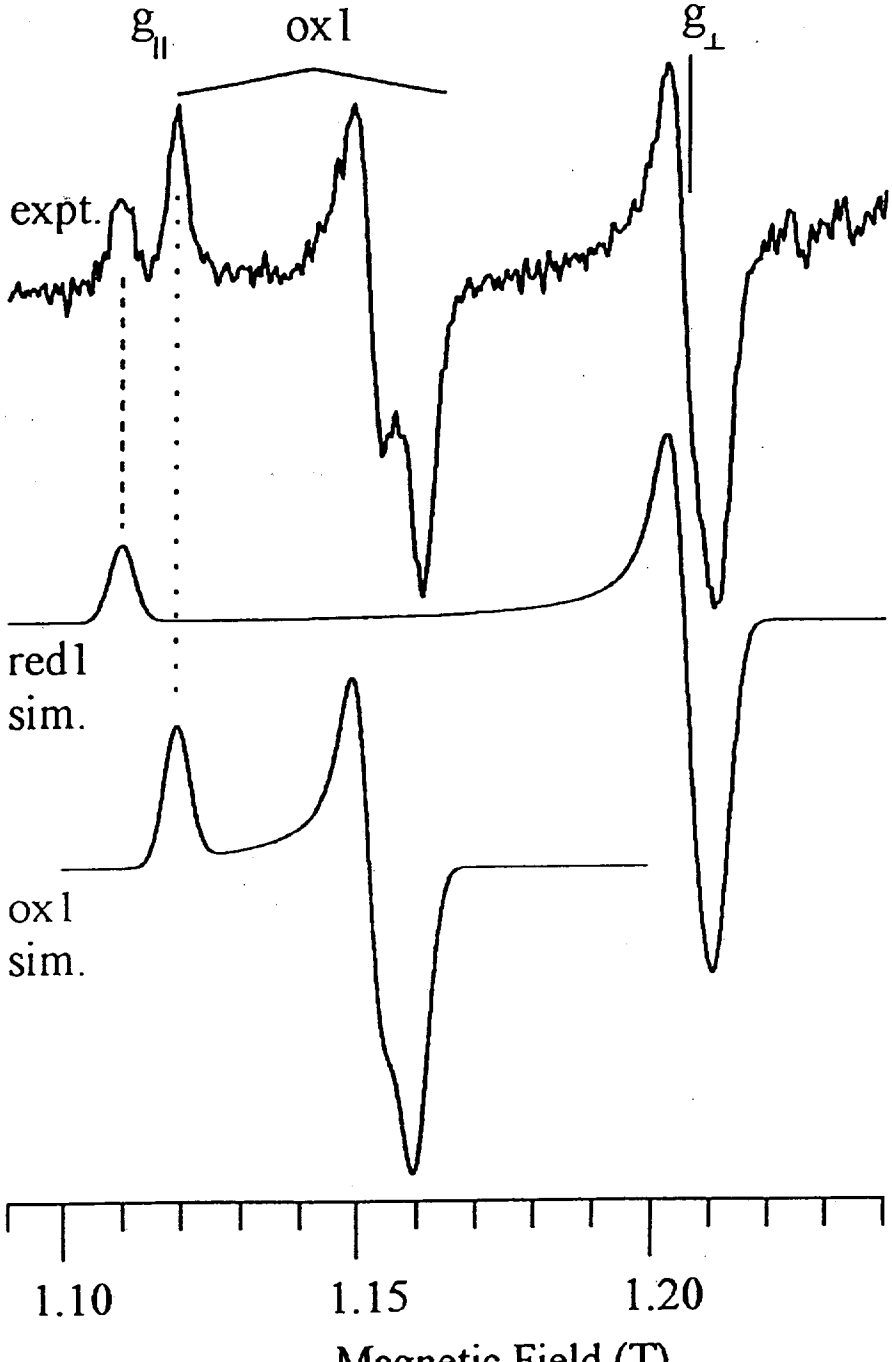
g||
ox1
g⊥
expt.
red1
sim.
ox1
sim.
1.10
1.15
1.20
Magnetic Field (T)